

PKS 2254+074: A Blazar in Likely Association with the Neutrino Event IceCube-190619A

SHUNHAO JI¹ AND ZHONGXIANG WANG^{1,2}

¹*Department of Astronomy, School of Physics and Astronomy, Yunnan University, Kunming 650091, China; jishunhao@mail.ynu.edu.cn; wangzx20@ynu.edu.cn*

²*Shanghai Astronomical Observatory, Chinese Academy of Sciences, 80 Nandan Road, Shanghai 200030, China*

ABSTRACT

We report our study of the field of a $\simeq 0.2$ PeV neutrino event IC-190619A. This neutrino belongs to Gold events, which more likely have an astrophysical origin. Among the two γ -ray sources within the neutrino's positional uncertainty region, we find that one of them, the BL-Lac-type blazar PKS 2254+074, had a γ -ray flare at the arrival time of the neutrino. The flare is determined to have lasted ~ 2.5 yr in a 180-day binned light curve, constructed from the data collected with the Large Area Telescope (LAT) onboard the *Fermi Gamma-ray Space Telescope (Fermi)*. Accompanying the flare, optical and mid-infrared brightening is also seen. In addition, ≥ 10 GeV high energy photons from the source have been detected, suggesting a hardening of the emission during the flare. Given both the positional and temporal coincidence of PKS 2254+074 with IC-190619A, we suggest that this blazar is likely another member of a few recently identified (candidate) neutrino-emitting blazars.

Keywords: Blazars (164); Gamma-ray sources (633); Neutrino astronomy (1100)

1. INTRODUCTION

The IceCube South Pole neutrino observatory (Aartsen et al. 2017) has been detecting neutrino events with energy from ~ 30 TeV to PeV since 2010 (IceCube Collaboration 2013). These high energy neutrinos have a high probability of arising from extraterrestrial sources. While the origin of such events had been under intense investigation, it was not until 2017 that the association of such an event, IceCube-170922A, and an extra-galactic source, the blazar TXS 0506+056, was established (IceCube Collaboration et al. 2018a,b). In addition, more recently the detection of the neutrino emission from the nearby Seyfert galaxy NGC 1068 at a significance of 4.2σ and that from the Galactic plane at a 4.5σ significance level have also been reported (IceCube Collaboration et al. 2022; Icecube Collaboration et al. 2023).

Blazars, the subclass of Active Galactic Nuclei (AGNs) with a relativistic jet pointing close to the line of sight, indeed have been suggested to be neutrino emitters (e.g., Kadler et al. 2016 and references therein). Protons possibly carried in a jet would interact with low-energy photons ($p\gamma$ interaction), and the produced pions decay and produce neutrinos and high-energy photons. One notable feature of the TXS 0506+056 case is that the blazar was undergoing a γ -ray flare; the peak flux reached $\simeq 5 \times 10^{-7}$ ph cm⁻² s⁻¹ in the en-

ergy of >0.1 GeV and the accompanying upto 400 GeV very-high-energy (VHE) emission was also observed (IceCube Collaboration et al. 2018a).

Following this identification, studies for connecting IceCube-detected neutrinos to blazars have been extensively carried out (e.g., Giommi et al. 2020a; Franckowiak et al. 2020; Stathopoulos et al. 2022; Plavin et al. 2023; Rodrigues et al. 2024). Among them, one is to find a flaring blazar that is positionally coincident with a reported neutrino event, which would strongly suggest the association between the two and thus enable the identification of the blazar as being a neutrino source. Thus far, the reported cases are PKS B1424–418 (Kadler et al. 2016), GB6 J1040+0617 (Garrappa et al. 2019), MG3 J225517+2409 (Franckowiak et al. 2020), GB6 J2113+1121 (Liao et al. 2022), PKS 0735+178 (Sahakyan et al. 2023), and NVSS J171822+423948 (Jiang et al. 2024). In addition, there are two other sources 1H 0323+342 and 3HSP J095507.9+355101; the former is a radio-loud narrow-line Seyfert galaxy in a minor γ -ray flare (Franckowiak et al. 2020) and the latter had an X-ray flare (Giommi et al. 2020b).

In our examination of neutrinos of high-probability astrophysical origin (i.e., Gold events that have signalness $\geq 50\%$; Abbasi et al. 2023), we noted a ~ 0.2 PeV track-like event IC-190619A. For its either originally reported

positional uncertainty region (IceCube Collaboration 2019) or that updated in the IceCube Event Catalog of Alert Tracks (IceCat-1; Abbasi et al. 2023), we could include the blazar PKS 2254+074 in it. This BL-Lac-type blazar has redshift $z = 0.19$ (Stickel et al. 1988; Peña-Herazo et al. 2021) and is a γ -ray source detected with the Large Area Telescope (LAT) onboard the *Fermi Gamma-ray Space Telescope (Fermi)* (e.g., Ballet et al. 2023). We also noted that this source had been in quiescence at γ -rays in most of the *Fermi*-LAT observation, but had a flare over the arrival time of IC-190619A. Thus, both the positional and temporal coincidence support that PKS 2254+074 is likely another neutrino-source case. We conducted analysis of the archival data for this blazar, and report the results in this paper. In this work, the cosmological parameters, $H_0 = 67.7 \text{ km s}^{-1} \text{ Mpc}^{-1}$, $\Omega_m = 0.31$, and $\Omega_\Lambda = 0.69$, from the Planck mission (Planck Collaboration et al. 2020) were used.

2. DATA ANALYSIS AND RESULTS

2.1. Positional coincidence analysis

On 2019 June 19 13:14:18.04 UT (MJD 58653.55), IceCube detected a ~ 0.2 PeV track-like event IC-190619A with signalness $\simeq 54.6\%$ ¹. The initial automated alert provided the arrival direction, which was subsequently updated from the more sophisticated reconstruction algorithms to be R.A. = $343^\circ.26_{-2.63}^{+4.08}$, Decl. = $+10^\circ.73_{-2.61}^{+1.51}$ (equinox J2000.0; IceCube Collaboration 2019). The blazar PKS 2254+074 (4FGL J2257.5+0748) is slightly outside the uncertainty region. However, when we added the systematic uncertainty often considered (e.g., Giommi et al. 2020a; Plavin et al. 2020; Hovatta et al. 2021; Sahakyan et al. 2023), the source is included in the combined uncertainty region (Figure 1). Furthermore in IceCat-1, the neutrino’s position was updated to be R.A. = $343^\circ.52_{-3.16}^{+4.13}$, Decl. = $+10^\circ.28_{-2.76}^{+2.02}$, having the blazar well enclosed (Figure 1).

No γ -ray sources in the LAT 8-year Source Catalog (at the time) were within the initial 90% statistical uncertainty region (IceCube Collaboration 2019). However in the latest *Fermi* LAT Source Catalog (i.e., 4FGL-DR4; Ballet et al. 2023), there is 4FGL J2306.6+0940, classified as blazar of uncertain type, also in the uncertainty region in IceCat-1. This source, as well as several other sources near but outside the error region (Figure 1), was fainter than 4FGL J2257.5+0748. The test statistic (TS) value for it was 48, which corresponds to

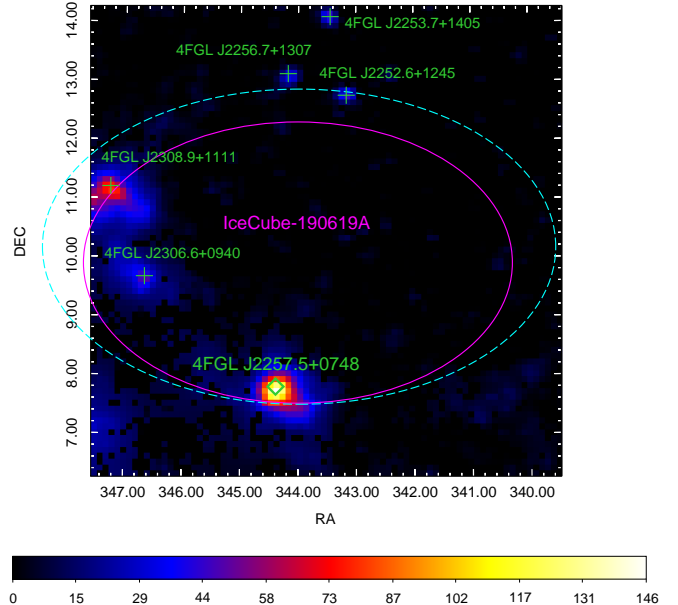


Figure 1. TS map of a size of $8^\circ \times 8^\circ$ centered at IC-190619A in the energy of 0.1–500 GeV. The dashed cyan ellipse marks the uncertainty region with the systematic uncertainty (by scaling the major and minor axis of the 90% error ellipse with a factor of 1.3; Giommi et al. 2020a) included, and the pink ellipse marks the uncertainty region given in IceCat-1. In addition to PKS 2254+074 (4FGL J2257.5+0748), another *Fermi* LAT source (4FGL J2306.6+0940) is also in the uncertainty region in IceCat-1.

the detection significance of 6.9σ ($\simeq \sqrt{TS}$). We checked its γ -ray light curve, and found it did not show any significant variations at the neutrino’s arrival time.

2.2. *Fermi*-LAT data analysis

2.2.1. Data and source model

The *Fermi*-LAT data used were 0.1–500 GeV photon events (evclass=128 and evtype=3) from the updated *Fermi* Pass 8 database in a time range of from 2008-08-04 15:43:36 (UTC) to 2024-04-18 00:05:53 (UTC). The region of interest (RoI) was set to be $20^\circ \times 20^\circ$ centered at PKS 2254+074. We excluded the events with zenith angles $> 90^\circ$ to avoid the Earth-limb contamination. The expression `DATA_QUAL > 0 && LAT_CONFIG = 1` was applied to select good time-interval events.

The source model was generated based on 4FGL-DR4. In the catalog, PKS 2254+074 (4FGL J2257.5+0748) was modeled as a point source with a power-law (PL) spectrum, $dN/dE = N_0(E/E_0)^{-\Gamma}$, where E_0 was fixed at 1.55 GeV. We adopted this spectral model. All

¹ https://gcn.gsfc.nasa.gov/notices_amon_g_b/132707_54984442.amon

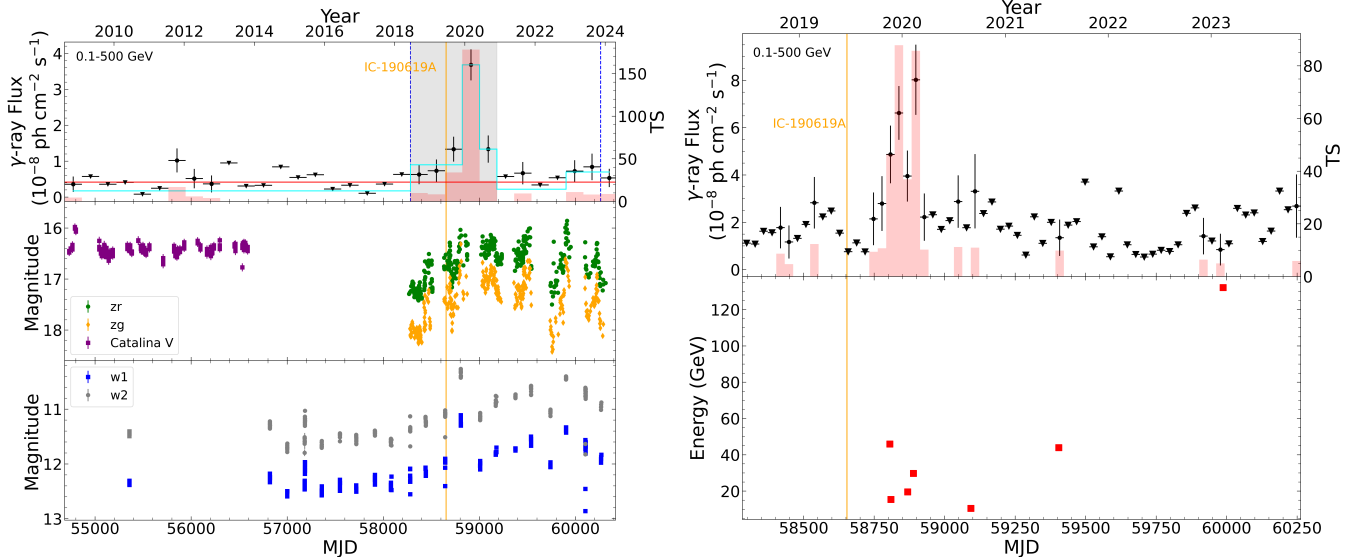


Figure 2. *Left:* 180-day binned γ -ray light curve of PKS 2254+074 in 0.1–500 GeV (upper), its optical Catalina *V* band and ZTF *zg* and *zr* band light curves (middle), and MIR WISE light curves (bottom). The orange line marks the arrival time of IC-190619A. In the top panel, the red line represents the average flux, the cyan histograms mark the blocks, and the gray region marks the flare defined by the HOP algorithm. *Right:* 30-day binned γ -ray light curve during the time period marked by the two blue dashed lines in the left panel (upper) and the arrival times of ≥ 10 GeV photons with probability $> 68\%$ (lower; see Section 2.2.3). In both γ -ray light curve panels, the downward triangles are the 95% C.L. flux upper limits and red histograms indicate the TS values of the data points.

other sources in 4FGL-DR4 within 25° of the target were included in the source model. The spectral indices and normalizations of the sources within 5° of the target were set as free parameters and the other parameters were fixed at the catalog values. The extragalactic diffuse emission and the Galactic diffuse emission components, `iso_P8R3_SOURCE_V3_v1.txt` and `gll_iem_v07.fits` respectively, were also included. Their normalizations were always set as free parameters in our analysis.

2.2.2. Light-curve analysis

Using the source model described above, we performed the standard binned likelihood analysis to the whole data in 0.1–500 GeV for PKS 2254+074. We obtained photon index $\Gamma = 2.18 \pm 0.08$, with a TS value of 136 ($\simeq 11.7\sigma$ detection significance). The results are consistent with those given in 4FGL-DR4.

We extracted the 0.1–500 GeV γ -ray light curve of the source by setting a 180-day time bin and performing the maximum likelihood analysis to the binned data. In the extraction, only the normalization parameters of the sources within 5° of the target were set free and the other parameters were fixed at the best-fit values obtained in the analysis of the whole data. For the data points with $\text{TS} < 4$, we computed the 95% confidence level (C.L.) upper limits. As revealed by the light curve (left panel of Figure 2), PKS 2254+074 had been nearly not de-

tectable for ~ 10 yr. Since 2018, a γ -ray flare peaking at $\sim \text{MJD } 58900$ was observed, during which IC-190619A was detected. To define the time duration of the flare, we employed the Bayesian block algorithm (Scargle et al. 2013) and HOP algorithm (Meyer et al. 2019), implemented through a python code² (Wagner et al. 2022). The start/end of a segment (e.g., a flare) is determined by the flux of a block exceeding above or dropping under the average flux (see details and the so-called HOP algorithm in Meyer et al. 2019). The duration determined is from MJD 58282.66 to 59182.66 (~ 2.5 yr), with the peak of the flare (the middle time of the highest-flux data point) being MJD 58912.66. For the time ranges excluding the flare, we defined them as the low state of the source.

We also constructed the optical and mid-infrared (MIR) light curves of PKS 2254+074 from the data taken respectively from the the Catalina Real-Time Transient Survey (Drake et al. 2009), the Zwicky Transient Facility (ZTF; Bellm et al. 2019), and the NEO-WISE Single-exposure Source Database (Mainzer et al. 2014). The optical bands are Catalina *V*, ZTF *g* and *r* (named as *zg* and *zr* respectively), and the MIR are WISE w1 ($3.4 \mu\text{m}$) and w2 ($4.6 \mu\text{m}$). The light curves show that the optical and MIR emissions accompanied

² <https://github.com/swagner-astro/lightcurves>

the γ -ray flare and brightened by ~ 1 mag. During the flare and afterwards, strong variations, with magnitude changes as large as ~ 1 , are also seen.

To show more details of the γ -ray flare, we further extracted a 30-day binned light curve from MJD 58282.66 to 60262.66 (P1; the region between the two blue dashed lines in the left panel of Figure 2); the same extraction process as the above was conducted. The light curve (right panel of Figure 2) further reveals a strong flaring activity, which lasted ~ 200 d from \sim MJD 58750 to 58950. During the time period, the peak flux reached $\sim 8 \times 10^{-8}$ ph cm $^{-2}$ s $^{-1}$.

2.2.3. Spectrum analysis

We performed the likelihood analysis to the data of the two states (i.e., the flare and low state) in 0.1–500 GeV. For the flare, the obtained best-fit $\Gamma = 2.06 \pm 0.07$ and photon flux $F_\gamma = (1.21 \pm 0.20) \times 10^{-8}$ ph cm $^{-2}$ s $^{-1}$ (TS $\simeq 190$ or detection significance $\simeq 13.8\sigma$). For the low state, $\Gamma = 2.24 \pm 0.15$ and $F_\gamma = (2.50 \pm 0.94) \times 10^{-9}$ ph cm $^{-2}$ s $^{-1}$ (TS $\simeq 38$ or detection significance $\simeq 6.2\sigma$). Because of the large uncertainties in the latter, no spectral changes between the two states could be determined.

We then obtained the γ -ray spectrum of PKS 2254+074 in the flare by performing the binned likelihood analysis to the data in 8 evenly divided energy bins in logarithm from 0.1 to 500 GeV. In this analysis, the spectral normalizations of the sources in the source model within 5° of the target were set free and all other spectral parameters of the sources were fixed at the values obtained in the above likelihood analysis to the data of the flare. For the spectrum, we only kept the data points with TS ≥ 4 .

For the low state, no decent spectrum can be obtained because of the low detection significance (i.e., TS $\simeq 38$).

Several blazars showed spectrum hardening during the flares that were temporally coincident with the neutrinos' arrival times (e.g., Garrappa et al. 2019; Giommi et al. 2020b; Liao et al. 2022), including TXS 0506+056 that emitted VHE photons (IceCube Collaboration et al. 2018a). We thus checked the high energy, ≥ 10 GeV photons from PKS 2254+074. Running `gtsrcprob` on the whole data in an 1° RoI with the best-fit model from the analysis of the whole data, we found five such photons with $>68\%$ probabilities. They were mostly during the flare. However, one had 132 GeV the highest energy with 95% probability, arrived after the flare on MJD 59987.38. The model used for the target can affect the estimation of photon probability. When using the best-fit model from the analysis of the P1 data (MJD 58282.66–60262.66),

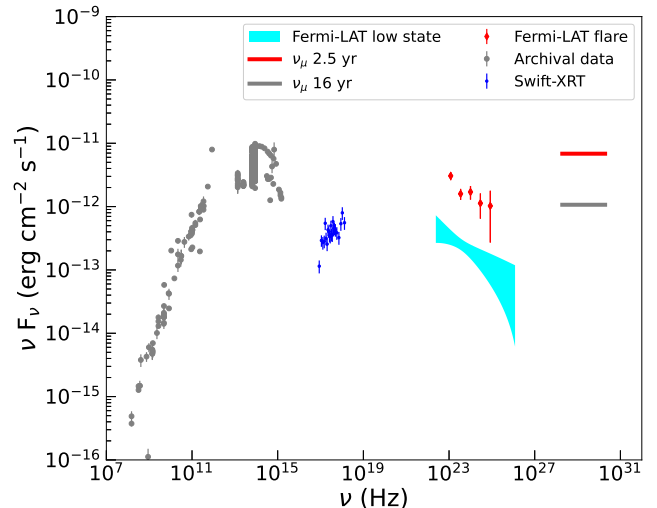


Figure 3. Broadband SED of PKS 2254+074. The gray dots are the archival data from Firmamento. The Swift-XRT X-ray spectrum is plotted as the blue dots. The γ -ray spectrum in the flare and the model fit in the low state are plotted as red diamonds and cyan region, respectively. The estimated neutrino fluxes for two time intervals (see Section 3) are shown as the red and gray lines.

we found seven high-energy photons, with probabilities $\geq 77\%$. The arrival times and energies of these photons are shown in the bottom right panel of Figure 2.

2.3. Broadband spectral energy distribution

We constructed the broadband spectral energy distribution (SED) of PKS 2254+074 from radio to γ -ray band. The archival radio to optical data were obtained using the tool Firmamento³. The X-ray spectral data points were extracted from the observations conducted with the X-ray Telescope (XRT) onboard the *Neil Gehrels Swift Observatory* (*Swift*). Details of the X-ray data and analysis are described in Appendix Section A. Both the γ -ray spectrum in the flare and the model fit in the low state are included in the SED (Figure 3).

3. DISCUSSION

Our analysis has found another blazar, PKS 2254+074, as a possible neutrino source. Its position is within the uncertainty region of the IceCube Gold event IC-190619A, and it had a flare temporally coincident with the arrival time of the neutrino. Such matches have established the likely association of a few blazars with neutrinos. In addition, we have detected several high-energy photons during the flare, which had not

³ https://firmamento.hosting.nyu.edu/data_access

been seen in the source’s long-term emission, suggesting the hardening of the source’s emission in the flare. This feature could be another similarity (Liao et al. 2022). We note that the peak flux of this blazar’s flare reached $\sim 8 \times 10^{-8} \text{ ph cm}^{-2} \text{ s}^{-1}$, which is also comparable with the values of those (candidate) neutrino blazars (Liao et al. 2022). These similarities strongly support the possibility of PKS 2254+074 as another member of the neutrino blazars.

PKS 2254+074 is classified as a low-synchrotron peaked (LSP) blazar in Ajello et al. (2022), and its peak frequency $\nu_{\text{pk}}^{\text{syn}} \simeq 4.0_{-2.0}^{+3.9} \times 10^{13} \text{ Hz}$ (given by Firmani using a machine learning estimator BLAST). Its long-term average γ -ray luminosity \mathcal{L}_γ and Γ we obtained are $3.7 \times 10^{44} \text{ erg s}^{-1}$ and 2.18, and during the (2.5 yr) flare, the values are $1.5 \times 10^{45} \text{ erg s}^{-1}$ and 2.06, respectively. Comparing it to the previously identified neutrino blazar candidates, it has the lowest redshift and the lowest long-term luminosity. The other neutrino blazars are generally in a redshift range of 0.3–1.5, but the very recently discovered one NVSS J171822+423948 has $z = 2.68$ (Jiang et al. 2024). Their γ -ray luminosities are in a range of $\sim 4 \times 10^{45}$ – 5×10^{48} . Thus, if it is truly a neutrino source, the detection could be due to its relatively close distance. The photon index and luminosity values of PKS 2254+074 are typical for a BL Lac (e.g., Ackermann et al. 2015; Chen 2018). Among the other neutrino blazars, GB6 J1040+0617 is in the same class, a BL Lac LSP. PKS B1424–418, GB6 J2113+1121, and NVSS J171822+423948 are also LSPs although they are flat-spectrum radio quasars (FSRQs). TXS 0506+056 and the other candidate 3HSP J095507.9+355101, which are an intermediate- and a high-synchrotron peaked blazars, respectively, have previously been noted as the outliers of the so-called blazar sequence (Giommi et al. 2020b). We also note that if we take the average \mathcal{L}_γ and $\nu_{\text{pk}}^{\text{syn}}$ values of PKS 2254+074, it could also be an outlier (because its $\mathcal{L}_\gamma < 10^{45} \text{ erg s}^{-1}$ while $\nu_{\text{pk}}^{\text{syn}} \simeq 4.0 \times 10^{13} \text{ Hz}$; see Figure 4 in Giommi et al. 2020b). Unfortunately, we do not have information for its $\nu_{\text{pk}}^{\text{syn}}$ in the flare. Whether its flaring variations are similar to those of TXS 0506+056 and 3HSP J095507.9+355101 are not known.

Following Giommi et al. (2020b) and Jiang et al. (2024), we estimated the neutrino flux given the detection of 1 muon neutrino event. Considering the effective area $A_{\text{eff}} \simeq 24 \text{ m}^2$ (GFU_Gold, see Abbasi et al. 2023), a PL neutrino energy spectrum with an index of -2 from 80 TeV to 8 PeV (Oikonomou et al. 2021), the integrated muon neutrino energy flux would be $3.2 \times 10^{-11} \text{ erg cm}^{-2} \text{ s}^{-1}$ and $4.9 \times 10^{-12} \text{ erg cm}^{-2} \text{ s}^{-1}$ (the corresponding differential spectra are shown in Fig-

ure 3), while the two values correspond to the neutrino-emitting time intervals of 2.5 yr (flare time duration) and 16 yr (approximate time length of the *Fermi*-LAT data), respectively. The corresponding luminosities \mathcal{L}_{ν_μ} would be $3.4 \times 10^{45} \text{ erg s}^{-1}$ and $5.4 \times 10^{44} \text{ erg s}^{-1}$, and the luminosity term $\epsilon_{\nu_\mu} L_{\nu_\mu}$ (see Giommi et al. 2020b), approximated with $\epsilon_{\nu_\mu} L_{\nu_\mu} \sim \mathcal{L}_{\nu_\mu} / \ln(8 \text{ PeV} / 80 \text{ TeV})$, would be $7.5 \times 10^{44} \text{ erg s}^{-1}$ and $1.2 \times 10^{44} \text{ erg s}^{-1}$, respectively.

The neutrino flux, on the other hand, may be estimated from the observed γ -ray flux (see Giommi et al. 2020b and Jiang et al. 2024 for detailed calculations). The connection between them is given as (Murase et al. 2018)

$$\begin{aligned} \epsilon_\nu L_{\epsilon_\nu} &\approx \frac{6(1+Y_{IC})}{5} \epsilon_\gamma L_{\epsilon_\gamma} \Big|_{\epsilon_{\text{syn}}^{p\pi}} \\ &\approx 8 \times 10^{44} \text{ erg s}^{-1} \left(\frac{\epsilon_\gamma L_{\epsilon_\gamma} \Big|_{\epsilon_{\text{syn}}^{p\pi}}}{7 \times 10^{44}} \right). \end{aligned} \quad (1)$$

Here, Y_{IC} is the Compton-Y parameter, typically ≤ 1 (Murase et al. 2018). Basically during the photopion ($p\pi$) process, three-eighths of the proton energy is taken away by all-flavour neutrinos and the remaining energy goes to the production of electrons and pionic γ -rays. Following Giommi et al. (2020b), we estimate the γ -ray luminosity term $\epsilon_\gamma L_\gamma \sim \mathcal{L}_\gamma / \ln(500 \text{ GeV} / 100 \text{ MeV}) \simeq 1.7 \times 10^{44} \text{ erg s}^{-1}$ (for 2.5 yr) or $\simeq 4.4 \times 10^{43} \text{ erg s}^{-1}$ (for 16 yr). Using Eq. 1, the muon neutrino luminosities (i.e., $\frac{1}{3} \epsilon_\nu L_{\epsilon_\nu}$) would be $6.7 \times 10^{43} \text{ erg s}^{-1}$ (2.5 yr) or $1.7 \times 10^{43} \text{ erg s}^{-1}$ (16 yr). Comparing the values with the above obtained by considering the detection of one muon neutrino with the IceCube, they are factors of 11 and 7, respectively, lower. The factors are approximately 4–14 times smaller than those estimated in the cases reported by Giommi et al. (2020b) and Jiang et al. (2024), but still indicate a low neutrino detection probability (i.e., the Poisson probability to detect one neutrino is ~ 0.1).

1 This work was based on observations obtained with
 2 the Samuel Oschin Telescope 48-inch and the 60-inch
 3 Telescope at the Palomar Observatory as part of the
 4 Zwicky Transient Facility project. ZTF is supported by
 5 the National Science Foundation under Grant No. AST-
 6 2034437 and a collaboration including Caltech, IPAC,
 7 the Weizmann Institute for Science, the Oskar Klein
 8 Center at Stockholm University, the University of Mary-
 9 land, Deutsches Elektronen-Synchrotron and Humboldt
 10 University, the TANGO Consortium of Taiwan, the
 11 University of Wisconsin at Milwaukee, Trinity College
 12 Dublin, Lawrence Livermore National Laboratories, and
 13 IN2P3, France. Operations are conducted by COO,
 14 IPAC, and UW.

15 This work made use of data products from the Wide-
 16 field Infrared Survey Explorer, which is a joint project
 17 of the University of California, Los Angeles, and the
 18 Jet Propulsion Laboratory/California Institute of Tech-
 19 nology, funded by the National Aeronautics and Space
 20 Administration.

21 We thank the referees for very detailed and help-
 22 ful comments. This research is supported by the
 23 Basic Research Program of Yunnan Province (No.
 24 202201AS070005), the National Natural Science Foun-
 25 dation of China (12273033), and the Original Inno-
 26 vation Program of the Chinese Academy of Sciences
 27 (E085021002). S.J. acknowledges the support of the sci-
 28 ence research program for graduate students of Yunnan
 29 University (KC-23234629).

REFERENCES

- Aartsen, M. G., Ackermann, M., Adams, J., et al. 2017,
 Journal of Instrumentation, 12, P03012,
 doi: [10.1088/1748-0221/12/03/P03012](https://doi.org/10.1088/1748-0221/12/03/P03012)
- Abbasi, R., Ackermann, M., Adams, J., et al. 2023, ApJS,
 269, 25, doi: [10.3847/1538-4365/acfa95](https://doi.org/10.3847/1538-4365/acfa95)
- Ackermann, M., Ajello, M., Atwood, W. B., et al. 2015,
 ApJ, 810, 14, doi: [10.1088/0004-637X/810/1/14](https://doi.org/10.1088/0004-637X/810/1/14)
- Ajello, M., Baldini, L., Ballet, J., et al. 2022, ApJS, 263,
 24, doi: [10.3847/1538-4365/ac9523](https://doi.org/10.3847/1538-4365/ac9523)
- Ballet, J., Bruel, P., Burnett, T. H., Lott, B., & The
 Fermi-LAT collaboration. 2023, arXiv e-prints,
 arXiv:2307.12546, doi: [10.48550/arXiv.2307.12546](https://doi.org/10.48550/arXiv.2307.12546)
- Bellm, E. C., Kulkarni, S. R., Graham, M. J., et al. 2019,
 PASP, 131, 018002, doi: [10.1088/1538-3873/aaecbe](https://doi.org/10.1088/1538-3873/aaecbe)
- Chen, L. 2018, ApJS, 235, 39,
 doi: [10.3847/1538-4365/aab8fb](https://doi.org/10.3847/1538-4365/aab8fb)
- Drake, A. J., Djorgovski, S. G., Mahabal, A., et al. 2009,
 ApJ, 696, 870, doi: [10.1088/0004-637X/696/1/870](https://doi.org/10.1088/0004-637X/696/1/870)
- Evans, P. A., Beardmore, A. P., Page, K. L., et al. 2009,
 MNRAS, 397, 1177,
 doi: [10.1111/j.1365-2966.2009.14913.x](https://doi.org/10.1111/j.1365-2966.2009.14913.x)
- Franckowiak, A., Garrappa, S., Paliya, V., et al. 2020, ApJ,
 893, 162, doi: [10.3847/1538-4357/ab8307](https://doi.org/10.3847/1538-4357/ab8307)
- Garrappa, S., Buson, S., Franckowiak, A., et al. 2019, ApJ,
 880, 103, doi: [10.3847/1538-4357/ab2ada](https://doi.org/10.3847/1538-4357/ab2ada)
- Giommi, P., Glauch, T., Padovani, P., et al. 2020a,
 MNRAS, 497, 865, doi: [10.1093/mnras/staa2082](https://doi.org/10.1093/mnras/staa2082)
- Giommi, P., Padovani, P., Oikonomou, F., et al. 2020b,
 A&A, 640, L4, doi: [10.1051/0004-6361/202038423](https://doi.org/10.1051/0004-6361/202038423)
- HI4PI Collaboration, Ben Bekhti, N., Flöer, L., et al. 2016,
 A&A, 594, A116, doi: [10.1051/0004-6361/201629178](https://doi.org/10.1051/0004-6361/201629178)
- Hovatta, T., Lindfors, E., Kiehlmann, S., et al. 2021, A&A,
 650, A83, doi: [10.1051/0004-6361/202039481](https://doi.org/10.1051/0004-6361/202039481)
- IceCube Collaboration. 2013, Science, 342, 1242856,
 doi: [10.1126/science.1242856](https://doi.org/10.1126/science.1242856)
- . 2019, GRB Coordinates Network, 24854, 1

- IceCube Collaboration, Aartsen, M. G., Ackermann, M., et al. 2018a, *Science*, 361, eaat1378, doi: [10.1126/science.aat1378](https://doi.org/10.1126/science.aat1378)
- . 2018b, *Science*, 361, 147, doi: [10.1126/science.aat2890](https://doi.org/10.1126/science.aat2890)
- IceCube Collaboration, Abbasi, R., Ackermann, M., et al. 2022, *Science*, 378, 538, doi: [10.1126/science.abg3395](https://doi.org/10.1126/science.abg3395)
- Icecube Collaboration, Abbasi, R., Ackermann, M., et al. 2023, *Science*, 380, 1338, doi: [10.1126/science.adc9818](https://doi.org/10.1126/science.adc9818)
- Jiang, X., Liao, N.-H., Wang, Y.-B., et al. 2024, *ApJL*, 965, L2, doi: [10.3847/2041-8213/ad36b9](https://doi.org/10.3847/2041-8213/ad36b9)
- Kadler, M., Krauß, F., Mannheim, K., et al. 2016, *Nature Physics*, 12, 807, doi: [10.1038/nphys3715](https://doi.org/10.1038/nphys3715)
- Liao, N.-H., Sheng, Z.-F., Jiang, N., et al. 2022, *ApJL*, 932, L25, doi: [10.3847/2041-8213/ac756f](https://doi.org/10.3847/2041-8213/ac756f)
- Mainzer, A., Bauer, J., Cutri, R. M., et al. 2014, *ApJ*, 792, 30, doi: [10.1088/0004-637X/792/1/30](https://doi.org/10.1088/0004-637X/792/1/30)
- Meyer, M., Scargle, J. D., & Blandford, R. D. 2019, *ApJ*, 877, 39, doi: [10.3847/1538-4357/ab1651](https://doi.org/10.3847/1538-4357/ab1651)
- Murase, K., Oikonomou, F., & Petropoulou, M. 2018, *ApJ*, 865, 124, doi: [10.3847/1538-4357/aada00](https://doi.org/10.3847/1538-4357/aada00)
- Oikonomou, F., Petropoulou, M., Murase, K., et al. 2021, *JCAP*, 2021, 082, doi: [10.1088/1475-7516/2021/10/082](https://doi.org/10.1088/1475-7516/2021/10/082)
- Peña-Herazo, H. A., Massaro, F., Gu, M., et al. 2021, *AJ*, 161, 196, doi: [10.3847/1538-3881/abe41d](https://doi.org/10.3847/1538-3881/abe41d)
- Planck Collaboration, Aghanim, N., Akrami, Y., et al. 2020, *A&A*, 641, A6, doi: [10.1051/0004-6361/201833910](https://doi.org/10.1051/0004-6361/201833910)
- Plavin, A., Kovalev, Y. Y., Kovalev, Y. A., & Troitsky, S. 2020, *ApJ*, 894, 101, doi: [10.3847/1538-4357/ab86bd](https://doi.org/10.3847/1538-4357/ab86bd)
- Plavin, A. V., Kovalev, Y. Y., Kovalev, Y. A., & Troitsky, S. V. 2023, *MNRAS*, 523, 1799, doi: [10.1093/mnras/stad1467](https://doi.org/10.1093/mnras/stad1467)
- Rodrigues, X., Paliya, V. S., Garrappa, S., et al. 2024, *A&A*, 681, A119, doi: [10.1051/0004-6361/202347540](https://doi.org/10.1051/0004-6361/202347540)
- Sahakyan, N., Giommi, P., Padovani, P., et al. 2023, *MNRAS*, 519, 1396, doi: [10.1093/mnras/stac3607](https://doi.org/10.1093/mnras/stac3607)
- Scargle, J. D., Norris, J. P., Jackson, B., & Chiang, J. 2013, arXiv e-prints, arXiv:1304.2818, doi: [10.48550/arXiv.1304.2818](https://doi.org/10.48550/arXiv.1304.2818)
- Stathopoulos, S. I., Petropoulou, M., Giommi, P., et al. 2022, *MNRAS*, 510, 4063, doi: [10.1093/mnras/stab3404](https://doi.org/10.1093/mnras/stab3404)
- Stickel, M., Fried, J. W., & Kuehr, H. 1988, *A&A*, 191, L16
- Wagner, S. M., Burd, P., Dorner, D., et al. 2022, in 37th International Cosmic Ray Conference, 868, doi: [10.22323/1.395.0868](https://doi.org/10.22323/1.395.0868)

APPENDIX

A. X-RAY DATA ANALYSIS

The X-ray data were from the observations conducted with Swift-XRT. There are six observations between 2007 and 2012, and the information is given in Table A1. We used the online Swift-XRT data products generator tool⁴ (for details about the online tool, see Evans et al. 2009) to extract the 0.3–10 keV spectrum of PKS 2254+074 from the six sets of the data. We grouped the spectrum to a minimum of 20 counts per bin using the GRPPHA task of FTOOLS. We fitted the spectrum with an absorbed PL model in the XSPEC 12.12.1, where the Galactic hydrogen column density N_{H} was fixed at $4.76 \times 10^{20} \text{ cm}^{-2}$ (HI4PI Collaboration et al. 2016). The obtained PL index was 1.87 ± 0.1 and unabsorbed flux was $1.36 \pm 0.12 \times 10^{-12} \text{ erg cm}^{-2} \text{ s}^{-1}$.

Table A1. Information for Swift-XRT observations

Date	Obsid	Exposure (ks)
2007-04-25	00036360001	5.01
2007-04-28	00036360002	4.41
2009-01-18	00036360003	4.02
2009-01-22	00036360004	2.06
2012-04-24	00036360005	0.38
2012-07-05	00036360006	0.63

⁴ https://www.swift.ac.uk/user_objects/